Chapter 15
Tug of War Optimization

15.1 Introduction

In this chapter, tug of war optimization (TWO) is presented as a newly developed nature-inspired, population-based metaheuristic algorithm. Utilizing a sport metaphor, the algorithm considers each candidate solution as a team participating in a series of rope-pulling competitions. The teams exert pulling forces on each other based on the quality of the solutions they represent. The competing teams move to their new positions according to the governing laws of motion from the Newtonian mechanics. Unlike many other metaheuristic methods, the algorithm is formulated in such a way that considers the qualities of both of the interacting teams. TWO is applicable to global optimization of discontinuous, multimodal, non-smooth, and non-convex functions.

This chapter consists of two parts. In the first part, the physical background and the basic rules of TWO are presented together with mathematical and engineering design problems in order to show the viability and efficiency of the algorithm [1].

In the second part, the algorithm is applied to different structural optimization problems including truss weight optimization with static constraints [1] and dynamic [2] constraints.

15.2 Tug of War Optimization Method

15.2.1 Idealized Tug of War Framework

Tug of war or rope pulling is a strength contest in which two competing teams pull on the opposite ends of a rope in an attempt to bring the rope in their direction against the pulling force of the opposing team. The activity dates back to ancient times and has continued to exist in different forms ever since. There has been a wide

A. Kaveh, *Advances in Metaheuristic Algorithms for Optimal Design of Structures*,
DOI 10.1007/978-3-319-46173-1_15

Fig. 15.1 A competing team in a tug of war competition

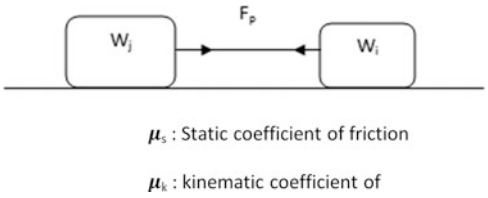

Fig. 15.2 An idealized tug of war framework

variety of rules and regulations for the game, but the essential part has remained almost unaltered. Naturally, as far as both teams sustain their grips of the rope, the movement of the rope corresponds to the displacement of the losing team. Figure 15.1 shows one of the competing teams in a tug of war competition.

Triumph in a real game of tug of war generally depends on many factors and could be difficult to analyze. However, an idealized framework is utilized here, where the two teams having weights W_i and W_j are considered as two objects lying on a smooth surface as shown in Fig. 15.2.

As a result of pulling the rope, the teams experience two equal and opposite forces (F_p) according to Newton's third law. For object i, as far as the pulling force is smaller than the maximum static friction force $(W_i\mu_s)$, the object rests in its place. Otherwise, the nonzero resultant force can be calculated as:

$$F_r = F_p - W_i\mu_k \tag{15.1}$$

As a result, the object i accelerates toward the object j according to the Newton's second law:

$$a = \frac{F_r}{\left({}^{W_i}/_{g}\right)} \tag{15.2}$$

Since the object i starts from zero velocity, its new position can be determined as:

$$X_i^{new} = \frac{1}{2}at^2 + X_i^{old} \tag{15.3}$$

15.2.2 Tug of War Optimization Algorithm

TWO is a population-based metaheuristic algorithm, which considers each candidate solution $X_i = \{x_{i,j}\}$ as a team engaged in a series of tug of war competitions. The weight of the teams is determined based on the quality of the corresponding solutions, and the amount of pulling force that a team can exert on the rope is assumed to be proportional to its weight. Naturally, the opposing team will have to maintain at least the same amount of force in order to sustain its grip of the rope. The lighter team accelerates toward the heavier team, and this forms the convergence operator of the TWO. The algorithm improves the quality of the solutions iteratively by maintaining a proper exploration/exploitation balance using the described convergence operator. The steps of TWO can be stated as follows:

Step 1: Initialization A population of N initial solutions is generated randomly:

$$x_{ij}^0 = x_{j,\min} + rand\left(x_{j,\max} - x_{j,\min}\right) \qquad j = 1, 2, \ldots, n \tag{15.4}$$

where x_{ij}^0 is the initial value of the jth variable of the ith candidate solution; $x_{j,\max}$ and $x_{j,\min}$ are the maximum and minimum permissible values for the jth variable, respectively; *rand* is a random number from a uniform distribution in the interval [0, 1]; and n is the number of optimization variables.

Step 2: Evaluation of Candidate Designs and Weight Assignment The objective function values for the candidate solutions are evaluated. All of the initial solutions are sorted and recorded in a memory denoted as the league. Each solution is considered as a team with the following weight:

$$W_i = \left(\frac{fit(i) - fit_{worst}}{fit_{best} - fit_{worst}}\right) + 1 \qquad i = 1, 2, \ldots, N \tag{15.5}$$

where *fit(i)* is the fitness value for the ith particle, evaluated as the penalized objective function value for constrained problems and fit_{best} and fit_{worst} are the fitness values for the best and worst candidate solutions of the current iteration. According to Eq. (15.5), the weights of the teams range between 1 and 2.

Step 3: Competition and Displacement In TWO each of the teams of the league competes against all the others one at a time to move to its new position in each iteration. The pulling force exerted by a team is assumed to be equal to its static

friction force ($W\mu_s$). Hence, the pulling force between teams i and j ($F_{p,ij}$) can be determined as $\max\{W_i\mu_s, W_j\mu_s\}$. Such a definition keeps the position of the heavier team unaltered.

The resultant force affecting team i due to its interaction with heavier team j in the kth iteration can then be calculated as follows:

$$F_{r,ij}^k = F_{p,ij}^k - W_i^k \mu_k \tag{15.6}$$

where $F_{p,ij}^k$ is the pulling force between teams i and j in the kth iteration and μ_k is the coefficient of kinematic friction. Consequently, team i accelerates toward team j:

$$a_{ij}^k = \left(\frac{F_{r,ij}^k}{W_i^k \mu_k}\right) g_{ij}^k \tag{15.7}$$

where a_{ij}^k is the acceleration of team i toward team j in the kth iteration and g_{ij}^k is the gravitational acceleration constant defined as:

$$g_{ij}^k = X_j^k - X_i^k \tag{15.8}$$

where X_j^k and X_i^k are the position vectors for candidate solutions j and i in the kth iteration, respectively. Finally, the displacement of the team i after competing with team j can be derived as:

$$\Delta X_{ij}^k = \frac{1}{2} a_{ij}^k \Delta t^2 + \alpha^k \beta (X_{\max} - X_{\min}) \circ randn\,(1, n) \tag{15.9}$$

The second term of Eq. (15.9) introduces randomness into the algorithm. This term can be interpreted as the random portion of the search space traveled by team i before it stops after the applied force is removed. The role of α^k is to gradually decrease the random portion of the team's movement. For most of the applications, α could be considered as a constant chosen from the interval [0.9, 0.99]; bigger values of α decrease the convergence speed of the algorithm and help the candidate solutions explore the search space more thoroughly. β is a scaling factor which can be chosen from the interval (0,1]. This parameter controls the steps of the candidate solutions when moving in the search space. When the search space is supposed to be searched more accurately with smaller steps, smaller values should be chosen for this parameter. For our numerical examples, values between 0.01 and 0.05 seem to be appropriate for this parameter; $X_{\max}$ and $X_{\min}$ are the vectors containing the upper and lower bounds of the permissible ranges of the design variables, respectively; $\circ$ denotes element-by-element multiplication; and $randn\,(1, n)$ is a vector of random numbers drawn from a standard normal distribution.

It should be noted that when team j is lighter than team i, the corresponding displacement of team i will be equal to zero (i.e., ΔX_{ij}^k). Finally, the total displacement of team i in iteration k is equal to (i not equal j):

$$\Delta X_i^k = \sum_{j=1}^{N} \Delta X_{ij}^k \tag{15.10}$$

The new position of the team i at the end of the kth iteration is then calculated as:

$$X_i^{k+1} = X_i^k + \Delta X_i^k \tag{15.11}$$

Step 4: Updating the League Once the teams of the league compete against each other for a complete round, the league should be updated. This is done by comparing the new candidate solutions (the new positions of the teams) to the current teams of the league. That is to say, if the new candidate solution i is better than the Nth team of the league in terms of objective function value, the Nth team is removed from the league, and the new solution takes its place.

Step 5: Handling the Side Constraints It is possible for the candidate solutions to leave the search space, and it is important to deal with such solutions properly. This is especially the case for the solutions corresponding to lighter teams for which the values of ΔX are usually bigger. Different strategies might be used in order to solve this problem. In this chapter a new strategy is introduced and incorporated using the global best solution. The new value of the jth optimization variable of the ith team that violated side constraints in the kth iteration is defined as:

$$x_{ij}^k = GB_j + \left(\frac{randn}{k}\right)\left(GB_j - x_{ij}^{k-1}\right) \tag{15.12}$$

where GB_j is the jth variable of the global best solution (i.e., the best-so-far solution) and *randn* is a random number drawn from a standard normal distribution. There is a very slight possibility for the newly generated variable to be still outside the search space. In such cases a flyback strategy is used.

The abovementioned strategy is utilized with a certain probability (0.5 in this chapter). For the rest of the cases, the violated limit is taken as the new value of the jth optimization variable.

Step 6: Termination Steps 2 through 5 are repeated until a termination criterion is satisfied. The pseudo code of TWO is presented in Table 15.1.

Table 15.1 Pseudo code of the TWO algorithm developed in this study

```
procedure Tug of War Optimization
begin
    Initialize parameters;
    Initialize a population of N random candidate solutions;
    Initialize the league by recording all random candidate solution;
    while (termination condition not met) do
        Evaluate the objective function values for the candidate solutions
        Sort the new solutions and update the league
        Define the weights of the teams of the league W_i based on fit(X_i)
            for each team i
            for each team j
                if (W_i < W_j)
                    Move team i towards team j using Eq. (15.9);
                end if
            end for
            Determine the total displacement of team i using Eq. (15.10)
            Determine the final position of team i using Eq.(15.11)
            Use the side constraint handling technique to regenerate violating variables
        end for
    end while
end
```

15.3 Mathematical and Engineering Design Problems

In order to evaluate the efficiency of the proposed algorithm, some benchmark mathematical and engineering design test problems are considered from the literature. A set of unimodal and multimodal mathematical optimization problems are studied in Sect. 15.3.1. In addition, two well-studied engineering design problems are investigated in Sect. 15.3.2. A population of 20 agents and a maximum number of permitted iterations of 200 are used for all test problems. The coefficient of static friction (μ_s) is taken as unity, while the coefficient of kinematic friction (μ_k) varies linearly from 1 to 0.1. Since smaller values of μ_k let the teams slide more easily toward each other and vice versa, such a parameter selection helps the algorithm's agents to explore the search space at early iterations without being severely affected by each other. As the optimization process proceeds, the values of μ_k gradually decrease allowing for convergence. It was found that using the same value of kinematic friction coefficient for all teams yields the best optimization results for TWO.

15.3.1 Mathematical Optimization Problems

In this section the efficiency of TWO is evaluated by solving the mathematical benchmark problems summarized in Table 15.2. These benchmark problems are taken from [3], where some variants of GA were used as the optimization algorithm. The results obtained by TWO are presented in Table 15.3 along with those of GA variants. Each objective function is optimized 50 times independently starting from different initial populations, and the average number of function evaluations required by each algorithm is presented. The numbers in the parentheses indicate the ratio of the successful runs in which the algorithm has located the global minimum with predefined accuracy, which is taken as $\varepsilon = f_{\min} - f_{final} = 10^{-4}$. The absence of the parentheses means that the algorithm has been successful in all independent runs.

As it can be seen from Table 15.3, TWO generally performs better than GA and its variants in the mathematical optimization problems considered in this study.

15.3.2 Engineering Design Problems

In order to further investigate the efficiency of the TWO, two engineering design problems are considered in this section. These problems have been previously studied using different optimization algorithms. The constrained optimization problems are turned into unconstrained ones using a penalty approach. If the constraints are satisfied, then the amount of penalty will be zero; otherwise, its value can be calculated as the ratio of violated constraint to the corresponding allowable limit.

15.3.2.1 Design of a Tension/Compression Spring

Weight minimization of the tension/compression spring shown in Fig. 15.3, subject to constraints on shear stress, surge frequency, and minimum deflection, is considered as the first engineering design example. This problem was first described by Belegundu [4] and Arora [5]. The design variables are the mean coil diameter D (x_1), the wire diameter $d(x_2)$, and the number of active coils $N(x_3)$.

The cost function can be stated as:

$$f_{\text{cost}}(\mathbf{X}) = (x_3 + 2)x_2x_1^2 \tag{15.13}$$

while the constraints are:

Table 15.2 Details of the benchmark mathematical problems solved in this study

Function name	Side constraints	Function	Global minimum
Aluffi-Pentini	$\mathbf{X} \in [-10, 10]^2$	$f(\mathbf{X}) = \frac{1}{4}x_1^4 - \frac{1}{2}x_1^2 + \frac{1}{10}x_1 + \frac{1}{2}x_2^2$	−0.352386
Bohachevsky 1	$\mathbf{X} \in [-100, 100]^2$	$f(\mathbf{X}) = x_1^2 + 2x_2^2 - \frac{3}{10}\cos(3\pi x_1) - \frac{4}{10}\cos(4\pi x_2) + \frac{7}{10}$	0.0
Bohachevsky 2	$\mathbf{X} \in [-50, 50]^2$	$f(\mathbf{X}) = x_1^2 + 2x_2^2 - \frac{3}{10}\cos(3\pi x_1)\cos(4\pi x_2) + \frac{3}{10}$	0.0
Becker and Lago	$\mathbf{X} \in [-10, 10]^2$	$f(\mathbf{X}) = \left(\lvert x_1\rvert - 5\right)^2 + \left(\lvert x_2\rvert - 5\right)^2$	0.0
Branin	$0 \le x_2 \le 15\ -5 \le x_1 \le 10$	$f(\mathbf{X}) = \left(x_2 - \frac{5.1}{4\pi^2}x_1^2 + \frac{5}{\pi}x_1\right)^2 + 10\left(1 - \frac{1}{8\pi}\right)\cos(x_1) + 10$	0.397887
Camel	$\mathbf{X} \in [-5, 5]^2$	$f(\mathbf{X}) = 4x_1^2 - 2.1x_1^4 + \frac{1}{3}x_1^6 + x_1x_2 - 4x_2^2 + 4x_2^4$	−1.0316
Cb3	$\mathbf{X} \in [-5, 5]^2$	$f(\mathbf{X}) = 2x_1^2 - 1.05x_1^4 + \frac{1}{6}x_1^6 + x_1x_2 + x_2^2$	0.0
Cosine mixture	$n = 4, \mathbf{X} \in [-1, 1]^n$	$f(\mathbf{X}) = \sum_{i=1}^{n} x_i^2 - \frac{1}{10}\sum_{i=1}^{n}\cos(5\pi x_i)$	−0.4
DeJoung	$\mathbf{X} \in [-5.12, 5.12]^3$	$f(\mathbf{X}) = x_1^2 + x_2^2 + x_3^2$	0.0
Exponential	$n = 2, 4, 8, \mathbf{X} \in [-1, 1]^n$	$f(\mathbf{X}) = -\exp\left(-0.5\sum_{i=1}^{n} x_i^2\right)$	−1
Goldstein and Price	$\mathbf{X} \in [-2, 2]^2$	$f(\mathbf{X}) = \left[1 + (x_1 + x_2 + 1)^2\left(19 - 14x_1 + 3x_1^2 - {}^1 14x_2 + 6x_1x_2 + 3x_2^2\right]\right.$ $\left.\times\left[30 + (2x_1 - 3x_2)^2\left(18 - 32x_1 + 12x_1^2 + 48x_2 - 36x_1x_2 + 27x_2^2\right]^2\right.\right.$	3.0
Griewank	$\mathbf{X} \in [-100, 100]^2$	$f(\mathbf{X}) = 1 + \frac{1}{200}\sum_{i=1}^{2} x_i^2 - \prod_{i=1}^{2}\cos\left(\frac{x_i}{\sqrt{i}}\right)$	0.0
Hartman 3	$\mathbf{X} \in [0, 1]^3$	$f(\mathbf{X}) = -\sum_{i=1}^{4} c_i \exp\left(-\sum_{j=1}^{3} a_{ij}\left(x_j - p_{ij}\right)^2\right)$ $a = \begin{bmatrix} 3 & 10 & 30 \\ 0.1 & 10 & 35 \\ 3 & 10 & 30 \\ 0.1 & 10 & 35 \end{bmatrix}$, $c = \begin{bmatrix} 1 \\ 1.2 \\ 3 \\ 3.2 \end{bmatrix}$ and $p = \begin{bmatrix} 0.3689 & 0.117 & 0.2673 \\ 0.4699 & 0.4387 & 0.747 \\ 0.1091 & 0.8732 & 0.5547 \\ 0.03815 & 0.5743 & 0.8828 \end{bmatrix}$.	−3.862782

Hartman 6	$\mathbf{X} \in [0,1]^6$	$f(\mathbf{X}) = -\sum_{i=1}^{4} c_i \exp\left(-\sum_{j=1}^{6} a_{ij}\left(x_j - p_{ij}\right)^2\right)$ $a = \begin{bmatrix} 10 & 3 & 17 & 3.5 & 1.7 & 8 \\ 0.05 & 10 & 17 & 0.1 & 8 & 14 \\ 3 & 3.5 & 17 & 10 & 17 & 8 \\ 17 & 8 & 0.05 & 10 & 0.1 & 14 \end{bmatrix}$, $c = \begin{bmatrix} 1 \\ 1.2 \\ 3 \\ 3.2 \end{bmatrix}$ and $p = \begin{bmatrix} 0.1312 & 0.1696 & 0.5569 & 0.0124 & 0.8283 & 0.5886 \\ 0.2329 & 0.4135 & 0.8307 & 0.3736 & 0.1004 & 0.9991 \\ 0.2348 & 0.1451 & 0.3522 & 0.2883 & 0.3047 & 0.6650 \\ 0.4047 & 0.8828 & 0.8732 & 0.5743 & 0.1091 & 0.0381 \end{bmatrix}$	-3.322368

Table 15.3 Performance comparison of TWO and GA variants in the mathematical optimization problems

Function name	GEN	GEN–S	GEN–S–M	GEN–S–M–LS	TWO [1]
AP	1360 (0.99)	1360	1277	1253	1092
Bf1	3992	3356	1640	1615	1404
Bf2	20,234	3373	1676	1636	1232
BL	19,596	2412	2439	1436	1216
Branin	1442	1418	1404	1257	1189
Camel	1358	1358	1336	1300	1212
Cb3	9771	2045	1163	1118	992
CM	2105	2105	1743	1539	1420
DeJoung	9900	3040	1462	1281	1346
Exp2	938	936	817	807	314
Exp4	3237	3237	2054	1496	815
Exp8	3237	3237	2054	1496	1257
Goldstein and Price	1478	1478	1408	1325	1690
Griewank	18,838 (0.91)	3111 (0.91)	1764	1652 (0.99)	1766
Hartman3	1350	1350	1332	1274	1026
Harman6	2562 (0.54)	2562 (0.54)	2530 (0.67)	1865 (0.68)	1601 (0.68)

Fig. 15.3 Schematic of the tension/compression spring

$$
\begin{aligned}
g_1(\mathbf{X}) &= 1 - \frac{x_2^3 x_3}{71785 x_1^4} \le 0 \\
g_2(\mathbf{X}) &= \frac{4x_2^2 - x_1 x_2}{12566\left(x_2 x_1^3 - x_1^4\right)} + \frac{1}{5108 x_1^2} - 1 \le 0 \\
g_3(\mathbf{X}) &= 1 - \frac{140.45 x_1}{x_2^2 x_3} \le 0 \\
g_4(\mathbf{X}) &= \frac{x_1 + x_2}{1.5} - 1 \le 0
\end{aligned}
\tag{15.14}
$$

The side constraints are defined as follows:

Table 15.4 Comparison of the optimization results obtained in the tension/compression spring problem

Methods	Optimal design variables			
	$x_1(d)$	$x_2(D)$	$x_3(N)$	f_{cost}
Belegundu [4]	0.050000	0.315900	14.250000	0.0128334
Arora [5]	0.053396	0.399180	9.185400	0.0127303
Coello [6]	0.051480	0.351661	11.632201	0.0127048
Coello and Montes [7]	0.051989	0.363965	10.890522	0.0126810
He and Wang [8]	0.051728	0.357644	11.244543	0.0126747
Montes and Coello [9]	0.051643	0.355360	11.397926	0.012698
Kaveh and Talatahari [10]	0.051865	0.361500	11.000000	0.0126432
Kaveh and Talatahari [11]	0.051744	0.358532	11.165704	0.0126384
Kaveh and Mahdavi [12]	0.051894	0.3616740	11.007846	0.0126697
TWO [1]	0.051592	0.354379	11.428784	0.0126671

$$\begin{aligned} 0.05 \leq x_1 \leq 2 \\ 0.25 \leq x_2 \leq 1.3 \\ 2 \leq x_3 \leq 15 \end{aligned} \tag{15.15}$$

This problem has been solved by Belegundu [4] using eight different mathematical optimization techniques. Arora [5] utilized a numerical optimization technique called a constraint correction at the constant cost to investigate the problem. Coello [6] and Coello and Montes [7] used a GA-based algorithm to solve the problem. He and Wang [8] used a coevolutionary particle swarm optimization (CPSO). Montes and Coello [9] used evolution strategies. Kaveh and Talatahari used improved ant colony optimization [10] and charged system search (CSS) [11]. Recently, the problem has been solved by Kaveh and Mahdavi [12] using colliding bodies optimization (CBO).

The optimization results obtained by TWO are presented in Table 15.4 along with those of other methods. It can be seen that TWO found the best design overall. It should be noted that some constraints are slightly violated by the designs in [10, 11]. Table 15.5 shows the statistical results obtained for 30 independent optimization runs.

15.3.2.2 Design of a Welded Beam

The second test problem regards the design optimization of the welded beam shown in Fig. 15.4. This problem has been used for testing different optimization methods. The aim is to minimize the total manufacturing cost subject to constraints on shear stress (τ), bending stress (σ), buckling load (P_c), and deflection (δ). The four design variables, namely, h (x_1), l (x_2), t (x_3), and b (x_4), are also shown in the figure.

The objective function can be mathematically stated as:

$$f_{\text{cost}}(\mathbf{X}) = 1.10471x_1^2x_2 + 0.04811x_3x_4(14.0 + x_2) \tag{15.16}$$

The optimization constraints are

$$\begin{aligned} g_1(\mathbf{X}) &= \tau(\{x\}) - \tau_{\max} \leq 0 \\ g_2(\mathbf{X}) &= \sigma(\{x\}) - \sigma_{\max} \leq 0 \\ g_3(\mathbf{X}) &= x_1 - x_4 \leq 0 \\ g_4(\mathbf{X}) &= 0.10471x_1^2 + 0.04811x_3x_4(14.0 + x_2) - 5.0 \leq 0 \\ g_5(\mathbf{X}) &= 0.125 - x_1 \leq 0 \\ g_6(\mathbf{X}) &= \delta(\{x\}) - \delta_{\max} \leq 0 \\ g_7(\mathbf{X}) &= P - P_c(\{x\}) \leq 0 \end{aligned} \tag{15.17}$$

where

Table 15.5 Comparison of statistical optimization results obtained in the tension/compression spring design problem

Methods	Best	Mean	Worst	Std dev
Belegundu [4]	0.0128334	N/A	N/A	N/A
Arora [5]	0.0127303	N/A	N/A	N/A
Coello [6]	0.0127048	0.012769	0.012822	3.9390e-5
Coello and Montes [7]	0.0126810	0.0127420	0.012973	5.9000e-5
He and Wang [8]	0.0126747	0.012730	0.012924	5.1985e-5
Montes and Coello [9]	0.012698	0.013461	0.016485	9.6600e-4
Kaveh and Talatahari [10]	0.0126432	0.012720	0.012884	3.4888e-5
Kaveh and Talatahari [11]	0.0126384	0.012852	0.013626	8.3564e-5
Kaveh and Mahdavi [12]	0.0126697	0.0127296	0.012881	5.00376e-5
TWO [1]	0.0126671	0.0129709	0.0135213	2.6125e-4

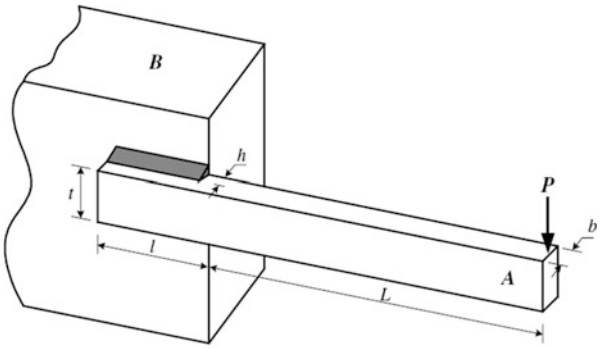

Fig. 15.4 Schematic of the welded beam

$$
\begin{aligned}
&\tau(\mathbf{X}) = \sqrt{(\tau')^2 + 2\tau'\tau''\frac{x_2}{2R} + (\tau'')^2} \\
&\tau' = \frac{P}{\sqrt{2}x_1x_2},\ \tau'' = \frac{MR}{J} \\
&M = P\left(L + \frac{x_2}{2}\right),\ R = \sqrt{\frac{x_2^2}{4} + \left(\frac{x_1 + x_3}{2}\right)^2} \\
&J = 2\left\{\sqrt{2}x_1x_2\left[\frac{x_2^2}{12} + \left(\frac{x_1+x_3}{2}\right)^2\right]\right\} \\
&\sigma(X) = \frac{6PL}{x_4x_3^2},\ \delta(X) = \frac{4PL^3}{Ex_3^3x_4} \\
&P_c(X) = \frac{4.013E\sqrt{\frac{x_3^2x_4^6}{36}}}{L^2}\left(1 - \frac{x_3}{2L}\sqrt{\frac{E}{4G}}\right) \\
&P = 6000lb,\ L = 14in \\
&E = 30 \times 10^6 psi,\ G = 12 \times 10^6 psi \\
&\tau_{\max} = 13.6 \times 10^3 psi,\ \sigma_{\max} = 30 \times 10^3 psi \\
&\delta_{\max} = 0.25in
\end{aligned}
\tag{15.18}
$$

The side constraints can be stated as:

$$0.1 \le x_1 \le 2,\ 0.1 \le x_2 \le 10,\ 0.1 \le x_3 \le 10,\ 0.1 \le x_4 \le 2 \tag{15.19}$$

Radgsdell and Phillips [13] utilized different optimization methods mainly based on mathematical programming to solve the problem and compared the results. GA-based methods are used by Deb [14], Coello [6], and Coello and Montes [7]. This test problem was also solved by He and Wang [8] using CPSO and Montes and Coello [9] using evolution strategies. Kaveh and Talatahari employed ant colony optimization [10] and charged system search [11]. Kaveh and Mahdavi [12] solved the problem using the colliding bodies optimization method.

Table 15.6 compares the best results obtained by the different optimization algorithms considered in this study. The statistical results for 30 independent runs are provided in Table 15.7. It can be seen from Table 15.6 that optimum design found by TWO is about 0.01 % heavier than that found by CBO which was the best design reported so far in literature.

15.4 Structural Optimization Problems

In this section the TWO is applied to different structural optimization problems including truss weight optimization with static [1] and dynamic constraints [2].

Table 15.6 Comparison of the optimization results obtained in the welded beam problem

Methods	Optimal design variables				
	$x_1(h)$	$x_2(l)$	$x_3(t)$	$x_4(b)$	f_{cost}
Radgsdell and Phillips [13]	0.2444	6.2189	8.2915	0.2444	2.3815
Deb [14]	0.248900	6.173000	8.178900	0.253300	2.433116
Coello [6]	0.208800	3.420500	8.997500	0.210000	1.748309
Coello and Montes [7]	0.205986	3.471328	9.020224	0.206480	1.728226
He and Wang [8]	0.202369	3.544214	9.048210	0.205723	1.728024
Montes and Coello [9]	0.199742	3.612060	9.037500	0.206082	1.737300
Kaveh and Talatahari [10]	0.205700	3.471131	9.036683	0.205731	1.724918
Kaveh and Talatahari [11]	0.205820	3.468109	9.038024	0.205723	1.724866
Kaveh and Mahdavi [12]	0.205722	3.47041	9.037276	0.205735	1.724663
TWO [1]	0.205728	3.47052	9.036631	0.205730	1.724855

Table 15.7 Comparison of statistical optimization results obtained in the welded beam problem

Methods	Best	Mean	Worst	Std Dev
Radgsdell and Phillips [13]	2.3815	N/A	N/A	N/A
Deb [14]	2.433116	N/A	N/A	N/A
Coello [6]	1.748309	1.771973	1.785835	0.011220
Coello and Montes [7]	1.728226	1.792654	1.993408	0.074713
He and Wang [8]	1.728024	1.748831	1.782143	0.012926
Montes and Coello [9]	1.737300	1.813290	1.994651	0.070500
Kaveh and Talatahari [10]	1.724918	1.729752	1.775961	0.009200
Kaveh and Talatahari [11]	1.724866	1.739654	1.759479	0.008064
Kaveh and Mahdavi [12]	1.724662	1.725707	1.725059	0.0002437
TWO [1]	1.724855	1.726016	1.729970	0.0009951

15.4.1 Truss Weight Optimization with Static Constraints

In this section, three truss weight optimization problems with constraints of stresses and displacements are presented. 30 agents are utilized for the first example, while 40 agents are used for the second and third examples. Maximum permissible iterations are considered as 400 for all examples.

15.4.1.1 Design of a Spatial 25-Bar Truss Structure

The spatial 25-bar truss schematized in Fig. 15.5 is the first structural design example. The material density and modulus of elasticity are 0.1 lb/in^3 and 10,000 ksi, respectively. Table 15.8 shows the two independent loading conditions applied to the structure. The 25 bars of the truss are classified into eight groups as follows:

(1) A_1, (2) A_2–A_5, (3) A_6–A_9, (4) A_{10}–A_{11}, (5) A_{12}–A_{13}, (6) A_{14}–A_{17}, (7) A_{18}–A_{21}, and (8) A_{22}–A_{25}.

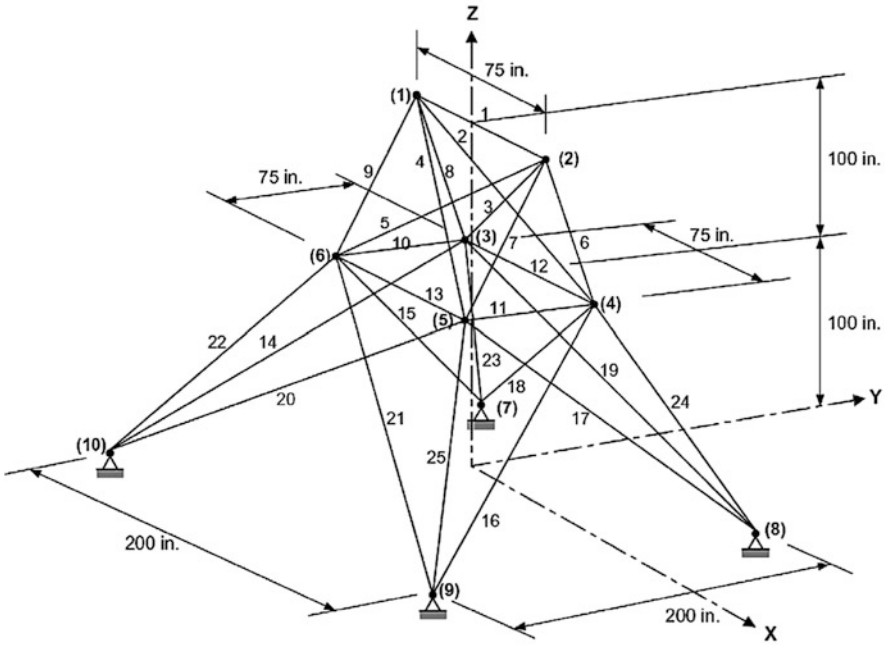

Fig. 15.5 Schematic of the spatial 25-bar truss structure

Table 15.8 Independent loading conditions acting on the spatial 25-bar truss

	Case 1			Case 2		
Node	P_x kips	P_y kips	P_z kips	P_x kips	P_y kips	P_z kips
1	0.0	20.0	−5.0	1.0	10.0	−5.0
2	0.0	−20.0	−5.0	0.0	10.0	−5.0
3	0.0	0.0	0.0	0.5	0.0	0.0
6	0.0	0.0	0.0	0.5	0.0	0.0

Maximum displacement limitations of 0.35 in are imposed on all nodes in all directions. The axial stress constraints, which are different for each group, are shown in Table 15.9. The cross-sectional areas vary continuously from 0.01 to 3.4 in^2 for all members.

Table 15.10 shows that the different optimization methods converged almost to the same structural weight. The best result obtained by TWO is 544.42 kg which is only slightly heavier than that of HS. However, it should be noted that according to our codes, the optimum design of HS slightly violates displacement constraints. Moreover, TWO requires 12,000 analyses to complete the optimization process, while HS has used 15000 analyses. The mean value and standard deviation of 30 independent optimization runs by TWO are 544.53 and 0.211 lb, respectively. Small differences in weight may be originated from the level of precision in the implementation of the optimization problem. For example, the displacement limit

Table 15.9 Member stress limits for the 25-bar spatial truss

Element group	Compressive stress limits ksi (MPa)	Tensile stress limit ksi (MPa)
1	35.092 (241.96)	40.0 (275.80)
2	11.590 (79.913)	40.0 (275.80)
3	17.305 (119.31)	40.0 (275.80)
4	35.092 (241.96)	40.0 (275.80)
5	35.092 (241.96)	40.0 (275.80)
6	6.759 (46.603)	40.0 (275.80)
7	6.959 (47.982)	40.0 (275.80)
8	11.082 (76.410)	40.0 (275.80)

Table 15.10 Comparison of the optimization results obtained in the spatial 25-bar truss problem

Element group		Optimal cross-sectional areas (in^2)			
		Rajeev and Krishnamoorthy, GA [15]	Schutte and Groenwold, PSO [16]	Lee and Geem, HS [17]	TWO [1]
1	A_1	0.10	0.010	0.047	0.010
2	A_2–A_5	1.80	2.121	2.022	1.979
3	A_6–A_9	2.30	2.893	2.950	2.993
4	A_{10}–A_{11}	0.20	0.010	0.010	0.010
5	A_{12}–A_{13}	0.10	0.010	0.014	0.010
6	A_{14}–A_{17}	0.80	0.671	0.688	0.684
7	A_{18}–A_{21}	1.80	1.611	1.657	1.678
8	A_{22}–A_{25}	3.0	2.717	2.663	2.656
Best weight (lb)		546	545.21	544.38	544.42
Average weight (lb)		N/A	546.84	N/A	544.53
Std dev (lb)		N/A	1.478	N/A	0.211
No. of analyses		N/A	9596	15,000	12,000

of 0.350 in set for TWO resulted in feasible optimized design reported in Table 15.10, yielding a maximum displacement of 0.3504 in which can be rounded to the abovementioned limit.

15.4.1.2 Design of a Spatial 72-Bar Truss Structure

A spatial 72-bar truss structure shown in Fig. 15.6 is considered as the second truss example. The two loading conditions acting on the structure are summarized in Table 15.11. The elements are grouped to form 16 design variables according to Table 15.12. The material density and the modulus of elasticity are taken as 0.1 lb/in^3 and 10,000 ksi, respectively. All members are subjected to a stress limitation of

±25 ksi. The displacements of the uppermost nodes along x- and y-axes are limited to ±0.25 in. Cross-sectional areas of bars can vary between 0.10 and 4.00 in^2, respectively.

This problem has been studied by Erbatur et al. [19] using genetic algorithms, Camp and Bichon [19] using ant colony optimization, Perez and Behdinan [20] using particle swarm optimization, Camp [21] using Big Bang–Big Crunch algorithm, and Kaveh and Khayatazad [22] using ray optimization, among others.

Table 15.12 compares the results obtained by the TWO to those previously reported in the literature. The weight of the best result obtained by TWO is 379.846 lb which is the best among the compared methods. Moreover, the mean weight of the results for 20 independent optimization runs of TWO is 381.98 lb which is less than all other methods. Also, TWO requires only 16,000 structural analyses while ACO, BB–BC, and RO require 18,500, 19,621, and 19,084, respectively.

15.4.1.3 Design of a 120-Bar Dome Truss

The third test problem in this section is the weight minimization of a 120-bar dome truss shown in Fig. 15.7. This structure was considered by Soh and Yang [23] as a configuration optimization problem. It has been solved by Lee and Geem [17], Kaveh and Talatahari [23], Kaveh et al. [24], Kaveh and Khayatazad [22], and Kaveh and Mahdavi [12] as a sizing optimization problem. The members of the structure are divided into seven groups as shown in Fig. 15.7.

The allowable tensile and compressive stresses are set according to the ASD-AISC (1989) provisions as follows:

$$\begin{cases} \sigma_i^+ = 0.6F_y & for \quad \sigma_i \geq 0 \\ \sigma_i^- & for \quad \sigma_i \leq 0 \end{cases} \tag{15.20}$$

where σ_i^- is the compressive allowable stress and depends on the elements slenderness ratio:

$$\sigma_i^- = \begin{cases} \left[\left(1 - \dfrac{\lambda_i^2}{2{C_c}^2}\right)F_y\right] \Big/ \left(\dfrac{5}{3} + \dfrac{3\lambda_i}{8C_c} - \dfrac{\lambda_i^3}{8C_c^3}\right) & for \quad \lambda_i \leq C_c \\ \dfrac{12\pi^2 E}{23\lambda_i^2} & for \quad \lambda_i \geq C_c \end{cases} \tag{15.21}$$

where E is the modulus of elasticity, F_y is the material's yield stress, λ_i is the slenderness ratio ($\lambda_i = \frac{K_i L_i}{r_i}$), K_i is the effective length factor, L_i is the member length, r_i is the radius of gyration, and C_c is the critical slenderness ratio separating elastic and inelastic buckling regions ($C_c = \sqrt{2\pi^2 E/F_y}$).

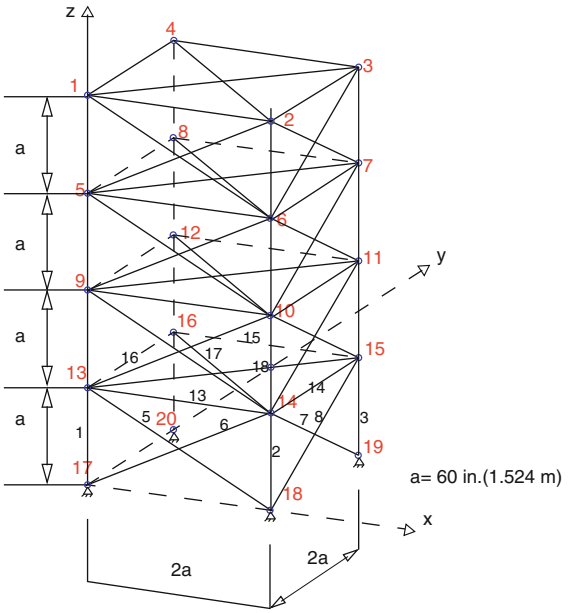

Fig. 15.6 Schematic of the spatial 72-bar truss structure

Table 15.11 Independent loading conditions acting on the spatial 72-bar truss

	Case 1			Case 2		
Node	P_x kips (kN)	P_y kips (kN)	P_z kips (kN)	P_x kips(kN)	P_y kips(kN)	P_z kips (kN)
1	5	5	−5	_	_	−5
2	–	–	–	–	–	−5
3	–	–	–	–	–	−5
4	–	–	–	–	–	−5

The modulus of elasticity and the material density are taken as 30,450 ksi (210 GPa) and 0.288 lb/in^3, respectively. The yield stress is taken as 58.0 ksi (400 MPa). The radius of gyration is expressed in terms of cross-sectional areas of the members as $r_i = aA_i^b$. Constants a and b depend on the types of sections adopted for the members such as pipes, angles, etc. In this example pipe sections are used for the bars for which a = 0.4993 and b = 0.6777. The dome is considered to be subjected to vertical loads at all unsupported nodes. These vertical loads are taken as −13.49 kips (60 kN) at node 1, −6.744 kips (30 kN) at nodes 2 through 14, and −2.248 kips (10 kN) at the other nodes. Four different problem variants are considered for this structure: with stress constraints and no displacement constraints (Case 1), with stress constraints and displacement limitations of ±0.1969 in (5 mm) imposed on all nodes in x and y directions (Case 2), no stress constraints and displacement limitations of ±0.1969 in (5 mm) imposed on all nodes in z direction

Table 15.12 Comparison of the optimization results obtained in the spatial 72-bar truss problem

Element group	Optimal cross-sectional areas (in^2)					
	Erbatur et al. [18]	Camp and Bichon [19]	Perez and Behdinan [20]	Camp [21]	Kaveh and Khayatazad [22]	TWO [1]
1–4	1.755	1.948	1.7427	1.8577	1.8365	1.9961
5–12	0.505	0.508	0.5185	0.5059	0.5021	0.5100
13–16	0.105	0.101	0.1000	0.1000	0.1000	0.1000
17–18	0.155	0.102	0.1000	0.1000	0.1004	0.1000
19–22	1.155	1.303	1.3079	1.2476	1.2522	1.2434
23–30	0.585	0.511	0.5193	0.5269	0.5033	0.5184
31–34	0.100	0.101	0.1000	0.1000	0.1002	0.1000
35–36	0.100	0.100	0.1000	0.1012	0.1001	0.1001
37–40	0.460	0.561	0.5142	0.5209	0.5730	0.5211
41–48	0.530	0.492	0.5464	0.5172	0.5499	0.5098
49–52	0.120	0.100	0.1000	0.1004	0.1004	0.1000
53–54	0.165	0.107	0.1095	0.1005	0.1001	0.1000
55–58	0.155	0.156	0.1615	0.1565	0.1576	0.1569
59–66	0.535	0.550	0.5092	0.5507	0.5222	0.5346
67–70	0.480	0.390	0.4967	0.3922	0.4356	0.3959
71–72	0.520	0.592	0.5619	0.5922	0.5971	0.5821
Best weight (lb)	385.76	380.24	381.91	379.85	380.458	379.846
Mean weight (lb)	N/A	383.16	N/A	382.08	382.553	381.976
Std dev (lb)	N/A	3.66	N/A	1.912	1.221	3.161
No. of analyses	N/A	18,500	N/A	19,621	19,084	16,000

(Case 3), and all the abovementioned constraints imposed together (Case 4). For Cases 1 and 2, the maximum cross-sectional area is taken as 5.0 in^2 (32.26 cm^2), while for Cases 3 and 4, it is taken as 20 in^2 (129.03 cm^2). The minimum cross-sectional area is taken as 0.775 in^2 (5 cm^2) for all cases.

Table 15.13 compares the results obtained by different optimization techniques for this example. It can be seen that the results found by TWO are comparable to those of other methods. In Case 1 the best result obtained by TWO is the same as that of CBO which is the best result so far. In Cases 3 and 4, the results obtained by TWO are better than those of RO, IRO, and CBO and are only slightly heavier than that of HPSACO (0.01 and 0.004 % in Cases 3 and 4, respectively). The average number of structural analyses required by the RO and IRO algorithms was reported as 19,900 and 18,300, respectively, while TWO uses 40 candidate solutions and

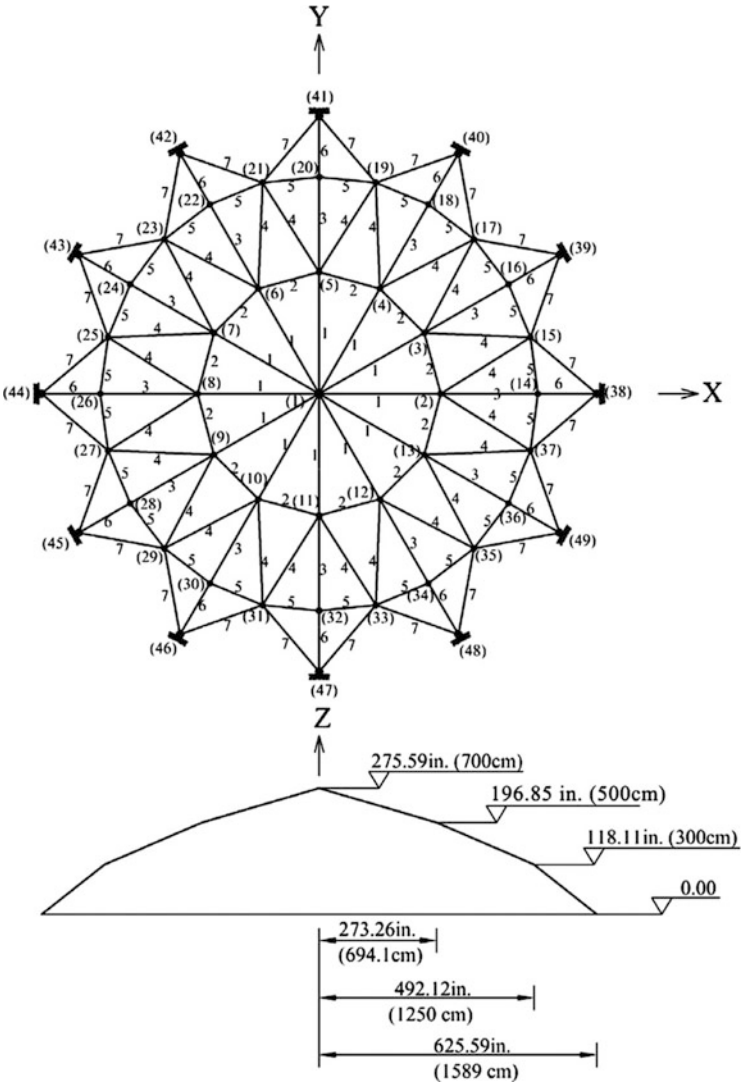

Fig. 15.7 Schematic of the 120-bar dome truss structure

400 iterations like CBO resulting in a maximum number of analyses of 16,000. HPSACO and HS, respectively, performed 10,000 and 35,000 structural analyses to obtain their optimal results. It should be noted that HPSACO is a hybrid method which combines good features of PSO, ACO, and HS.

Table 15.13 Comparison of the optimization results obtained in the 120-bar dome problem

Element group	Optimal cross-sectional areas (in^2)									
	Case 1					Case 2				
	HS (Lee and Geem [17])	HPSACO (Kaveh and Talatahari [23])	RO (Kaveh and Khayatazad [22])	CBO (Kaveh and Mahdavi [12])	TWO [1]	HS (Lee and Geem [17])	HPSACO (Kaveh and Talatahari [23])	RO (Kaveh and Khayatazad [22])	CBO (Kaveh and Mahdavi [12])	TWO [1]
1	3.295	3.311	3.128	3.1229	3.1229	3.296	3.779	3.084	3.0832	3.0831
2	3.396	3.438	3.357	3.3538	3.3538	2.789	3.377	3.360	3.3526	3.3526
3	3.874	4.147	4.114	4.1120	4.1120	3.872	4.125	4.093	4.0928	4.0928
4	2.571	2.831	2.783	2.7822	2.7822	2.570	2.734	2.762	2.7613	2.7613
5	1.150	0.775	0.775	0.7750	0.7750	1.149	1.609	1.593	1.5918	1.5923
6	3.331	3.474	3.302	3.3005	3.3005	3.331	3.533	3.294	3.2927	3.2927
7	2.784	2.551	2.453	2.4458	2.4458	2.781	2.539	2.434	2.4336	2.4336
Best weight (Ib)	19707.77	19491.3	19476.193	19454.7	19454.67	19893.34	20078.0	20071.9	20064.5	20064.86
Average weight (Ib)	–	–	–	19466.0	19454.98	–	–	–	20098.3	20106.85
Std dev (Ib)	–	–	33.966	7.02	1.17	–	–	112.135	26.17	116.15

(continued)

Table 15.13 (continued)

Element group	Optimal cross-sectional areas (in^2)								
	Case 3				Case 4				
	HPSACO (Kaveh and Talatahari [23])	RO (Kaveh and Khayatazad [22])	CBO (Kaveh and Mahdavi [12])	Present work [1]	HPSACO (Kaveh and Talatahari [23])	RO (Kaveh and Khayatazad [22])	IRO (Kaveh et al. [24])	CBO (Kaveh and Mahdavi [12])	TWO [1]
1	2.034	2.044	2.0660	1.9667	3.095	3.030	3.0252	3.0273	3.0247
2	15.151	15.665	15.9200	15.3920	14.405	14.806	14.8354	15.1724	14.7261
3	5.901	5.848	5.6785	5.7127	5.020	5.440	5.1139	5.2342	5.1338
4	2.254	2.290	2.2987	2.1960	3.352	3.124	3.1305	3.119	3.1369
5	9.369	9.001	9.0581	9.5439	8.631	8.021	8.4037	8.1038	8.4545
6	3.744	3.673	3.6365	3.6688	3.432	3.614	3.3315	3.4166	3.2946
7	2.104	1.971	1.9320	1.9351	2.499	2.487	2.4968	2.4918	2.4956
Best weight (Ib)	31670.0	31733.2	31724.1	31673.62	33248.9	33317.8	33256.48	33286.3	33250.31
Average weight (Ib)	–	–	32162.4	31680.34	–	–	–	33398.5	33282.64
Std dev (Ib)	–	274.991	240.22	6.15	–	354.333	–	67.09	25.38

15.4.2 Truss Weight Optimization with Dynamic Constraints

In this section weight minimization of truss structures with dynamic constraints using TWO is presented, where some of the natural frequencies of the structure are upper/lower bounded. Four numerical examples are provided in this section in order to examine the performance of TWO on frequency constraint weight minimization of truss structures. The results are compared to those of some other optimization techniques reported in the literature. A total population of 20 particles is considered for all of the examples except for the second example where 30 agents are used.

15.4.2.1 A 10-Bar Truss

Size optimization of a 10-bar truss structure shown in Fig. 15.8 is considered as the first dynamic constraint example. This is a well-known benchmark problem in the field of structural optimization subjected to frequency constraints. Cross-sectional areas of all ten members are assumed to be independent variables. A nonstructural mass of 454.0 kg is attached to all free nodes. Table 15.14 summarizes the material properties, variable bounds, and frequency constraints for this example.

This problem is addressed by different researchers using a wide variety of methods: Grandhi and Venkayya [25] using an optimality algorithm, Sedaghati et al. [26] utilizing a sequential quadratic programming and finite element force method, Wang et al. [27] using an evolutionary node shift method, Lingyun et al. [28] utilizing a niche hybrid genetic algorithm, Gomes employing particle swarm optimization algorithm [29], and Kaveh and Zolghadr employing standard and enhanced CSS [30], hybridized CSS–BBBC with trap recognition capability [31], democratic particle swarm optimization (DPSO) [32], and a hybridized PSRO [33].

Optimal structures found by different methods and the corresponding masses are summarized in Table 15.15. The optimal structure found by TWO is better than other methods and is only 0.05 % heavier than that of DPSO. It should be noted that the structures found by standard PSO [29] and CSS [30] are obtained using a modulus of elasticity of $E = 6.98 \times 10^{10}$ N/m^2, which generally results in lighter structures. Table 15.16 presents the natural frequencies of the optimized structures obtained by different methods. It can be seen that all constraints are satisfied. The mean value and the standard deviation of 50 independent runs of TWO are 539.28 kg and 3.28, respectively. Figure 15.9 presents the convergence curve of the best run of TWO for the 10-bar planar truss.

15.4.2.2 A 72-Bar Spatial Truss

A 72-bar spatial truss as depicted in Fig. 15.10 is presented as the second example. Four nonstructural masses of 2270 kg are attached to the uppermost four nodes. The shape of the structure is kept unchanged during the optimization process, and the

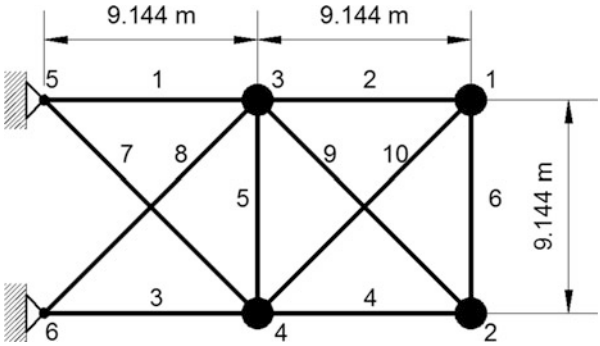

Fig. 15.8 Schematic of a 10-bar planar truss structure

Table 15.14 Material properties, variable bounds, and frequency constraints for the 10-bar truss structure

Property/unit	Value
E (modulus of elasticity)/N/m^2	6.89×10^{10}
ρ (material density)/kg/m^3	2770.0
Added mass/kg	454.0
Design variable lower bound/m^2	0.645×10^{-4}
Design variable upper bound/m^2	50×10^{-4}
L (main bar's dimension)/m	9.144
Constraints on the first three frequencies/Hz	$\omega_1 \geq 7$, $\omega_2 \geq 15$, $\omega_3 \geq 20$

design variables only include cross-sectional areas of the members, which are grouped into 16 groups. Material properties, variable bounds, frequency constraints, and added masses are listed in Table 15.17.

Optimized designs obtained by different optimization methods are summarized in Table 15.18. It should be mentioned that a modulus of elasticity of $E = 6.98 \times 1010$ N/m^2 is used by Gomes [29] and Kaveh and Zolghadr [30, 31]. This generally results in lighter structures. The mean value and the standard deviation of 50 independent runs of TWO are 336.1 kg and 5.8, respectively. Table 15.19 presents the first five natural frequencies for the optimized structures found by different methods. It could be seen that all of the frequency constraints are satisfied. Figure 15.11 presents the convergence curve for the best run of TWO.

15.4.2.3 A Simply Supported 37-Bar Planar Truss

Shape and size optimization of a simply supported 37-bar planar truss as shown in Fig. 15.12 is studied as the third example. The elements of the lower chord are modeled as bar elements with constant rectangular cross-sectional areas of 4×10^{-3} m^2. The rest of the members, which are modeled as bar elements, are grouped considering the symmetry. The y-coordinate of all the nodes on the upper chord can

Table 15.15 Optimal structures (cm^2) found by different methods for the planar 10-bar planar truss problem (the optimized weight does not include the added masses)

Element number	Grandhi and Venkayya [25]	Sedaghati et al. [26]	Wang et al. [27]	Lingyun et al. [28]	Gomes [29]	Kaveh and Zolghadr			
						Standard CSS [30]	DPSO [32]	PSRO [33]	TWO [2]
1	36.584	38.245	32.456	42.23	37.712	38.811	35.944	37.075	34.442
2	24.658	9.916	16.577	18.555	9.959	9.0307	15.530	15.334	14.861
3	36.584	38.619	32.456	38.851	40.265	37.099	35.285	33.665	36.485
4	24.658	18.232	16.577	11.222	16.788	18.479	15.385	14.849	15.564
5	4.167	4.419	2.115	4.783	11.576	4.479	0.648	0.645	0.669
6	2.070	4.419	4.467	4.451	3.955	4.205	4.583	4.643	4.606
7	27.032	20.097	22.810	21.049	25.308	20.842	23.610	24.528	23.086
8	27.032	24.097	22.810	20.949	21.613	23.023	23.599	23.188	24.527
9	10.346	13.890	17.490	10.257	11.576	13.763	13.135	12.436	13.013
10	10.346	11.452	17.490	14.342	11.186	11.414	12.357	13.500	12.686
Weight (kg)	594.0	537.01	553.8	542.75	537.98	531.95	532.39	532.85	532.68

Table 15.16 Natural frequencies (Hz) of the optimized designs for the 10-bar planar truss

Frequency number	Grandhi and Venkayya [25]	Sedaghati et al. [26]	Wang et al. [27]	Lingyun et al. [28]	Gomes [29]	Kaveh and Zolghadr			
						Standard CSS [30]	DPSO [31]	PSRO [32]	TWO [2]
1	7.059	6.992	7.011	7.008	7.000	7.000	7.000	7.000	7.001
2	15.895	17.599	17.302	18.148	17.786	17.442	16.187	16.143	16.185
3	20.425	19.973	20.001	20.000	20.000	20.031	20.000	20.000	20.001
4	21.528	19.977	20.100	20.508	20.063	20.208	20.021	20.032	20.018
5	28.978	28. 173	30.869	27.797	27.776	28.261	28.470	28.469	28.572
6	30.189	31.029	32.666	31.281	30.939	31.139	29.243	29.485	29.265
7	54.286	47.628	48.282	48.304	47.297	47.704	48.769	48.440	48.560
8	56.546	52.292	52.306	53.306	52.286	52.420	51.389	51.157	51.290

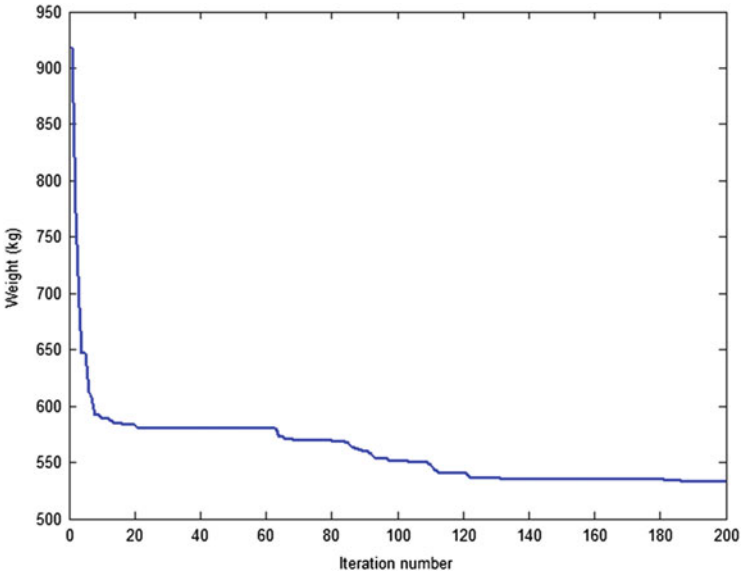

Fig. 15.9 Convergence curve of the best run of TWO for the 10-bar planar truss

vary in a symmetrical manner to form the shape variables. A nonstructural mass of 10 kg is attached to all free nodes of the lower chord. Constraints are imposed on the first three natural frequencies of the structure.

This example has been investigated by different researchers including Wang et al. [27] using an evolutionary node shift method, Lingyun et al. [28] using a niche hybrid genetic algorithm, Gomes [29] utilizing particle swarm algorithm, and Kaveh and Zolghadr using CSS [30], democratic PSO [32], and a hybridized PSRO algorithm [33]. Material properties, frequency constraints, added masses, and variable bounds for this example are listed in Table 15.20. Final cross-sectional areas and node coordinates obtained by different methods together with the corresponding weights are shown in Table 15.21.

Table 15.21 shows that TWO has obtained the best result among the algorithms. The mean weight and the standard deviation of 50 independent runs of TWO are 363.75 kg and 2.48 kg, respectively. Table 15.22 presents the first five natural frequencies of the optimized structures. Figure 15.13 presents the convergence curve of the best run of TWO for the simply supported 37-bar planar truss.

15.4.2.4 A 52-Bar Dome-Like Truss

As the last example, simultaneous shape and size optimization of a 52-bar dome-like truss is considered. The initial layout of the structure is depicted in Fig. 15.14. Nonstructural masses of 50 kg are attached to all free nodes. Material properties, frequency constraints, and variable bounds for this example are summarized in

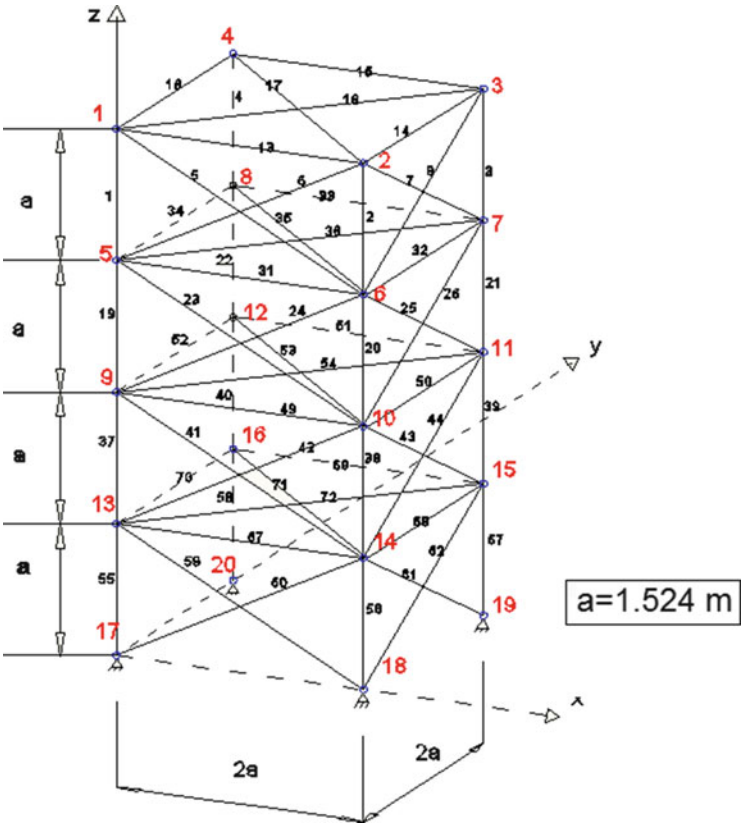

Fig. 15.10 The 72-bar spatial truss

Table 15.17 Material properties and frequency constraints for the 72-bar spatial truss

Property/unite	Value
E (modulus of elasticity)/N/m^2	6.89×10^{10}
ρ (material density)/kg/m^3	2770.0
Added mass/kg	2270
Design variable lower bound/m^2	0.645×10^{-4}
Constraints on the first three frequencies/Hz	$\omega_1 = 4.0$, $\omega_3 \geq 6$

Table 15.23. The elements of the structure are categorized in eight groups according to Table 15.24. All free nodes are permitted to move ±2 m from their initial position in a symmetrical manner.

This example has been solved by Lin et al. [34] using a mathematical programming technique and Lingyun et al. [28] using a niche hybrid genetic algorithm. Gomes [29] has studied the problem using particle swarm optimization algorithm. The authors have studied the problem using CSS [30], hybridized CSS–BBBC with

Table 15.18 Optimal cross-sectional areas for the 72-bar space truss (cm^2)

Group number	Elements	Sedaghati [26]	Gomes [29]	Kaveh and Zolghadr				
				Standard CSS[30]	Enhanced CSS[31]	CSS–BBBC[32]	PSRO [33]	TWO [2]
1	1–4	3.499	2.987	2.528	2.252	2.854	3.840	3.380
2	5–12	7.932	7.849	8.704	9.109	8.301	8.360	8.086
3	13–16	0.645	0.645	0.645	0.648	0.645	0.645	0.647
4	17–18	0.645	0.645	0.645	0.645	0.645	0.699	0.646
5	19–22	8.056	8.765	8.283	7.946	8.202	8.817	8.890
6	23–30	8.011	8.153	7.888	7.703	7.043	7.697	8.136
7	31–34	0.645	0.645	0.645	0.647	0.645	0.645	0.654
8	35–36	0.645	0.645	0.645	0.646	0.645	0.651	0.647
9	37–40	12.812	13.450	14.666	13.465	16.328	12.136	13.097
10	41–48	8.061	8.073	6.793	8.250	8.299	8.839	8.101
11	49–52	0.645	0.645	0.645	0.645	0.645	0.645	0.663
12	53-54	0.645	0.645	0.645	0.646	0.645	0.645	0.646
13	55–58	17.279	16.684	16.464	18.368	15.048	17.059	16.483
14	59–66	8.088	8.159	8.809	7.053	8.268	7.427	7.873
15	67–70	0.645	0.645	0.645	0.645	0.645	0.646	0.651
16	71–72	0.645	0.645	0.645	0.646	0.645	0.645	0.657
	Weight (kg)	327.605	328.823	328.814	328.393	327.507	329.80	328.83

Table 15.19 Natural frequencies (Hz) obtained by different methods for the 72-bar space truss

Frequency number	Sedaghati [26]	Gomes [29]	Kaveh and Zolghadr				
			Standard CSS [30]	Enhanced CSS [31]	CSS–BBBC [32]	PSRO [33]	TWO [2]
1	4.000	4.000	4.000	4.000	4.000	4.000	4.000
2	4.000	4.000	4.000	4.000	4.000	4.000	4.000
3	6.000	6.000	6.006	6.004	6.004	6.000	6.000
4	6.247	6.219	6.210	6.155	6.2491	6.418	6.259
5	9.074	8.976	8.684	8.390	8.9726	9.143	9.082

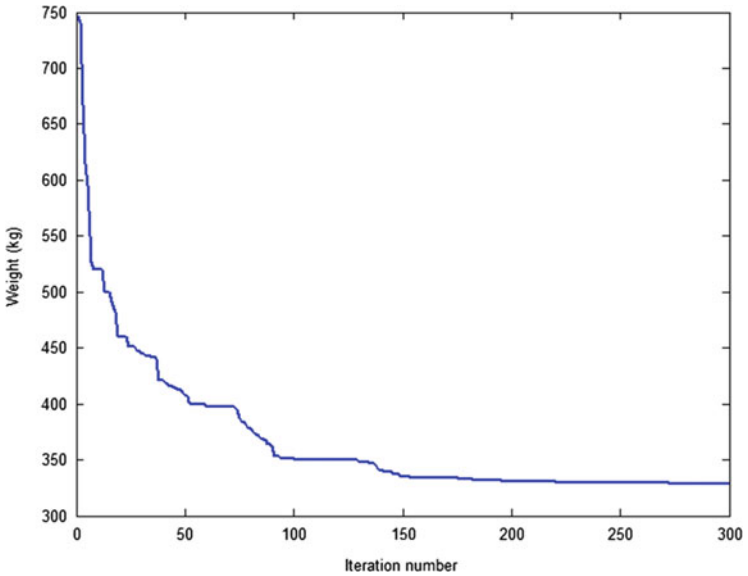

Fig. 15.11 Convergence curve of the best run of TWO for the 72-bar planar truss

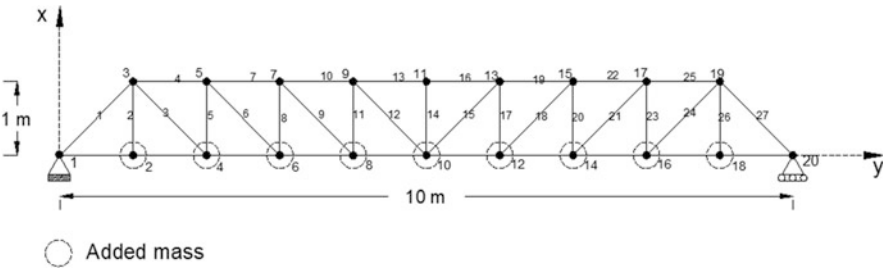

Fig. 15.12 A simply supported planar 37-bar truss

Table 15.20 Material properties, frequency constraints, and variable bounds for the simply supported 37-bar planar truss

Property/unit	Value
E (modulus of elasticity)/N/m^2	2.1×10^{11}
ρ (material density)/kg/m^3	7800
Design variable lower bound/m^2	1×10^{-4}
Design variable upper bound/m^2	10×10^{-4}
Added mass/kg	10
Constraints on the first three frequencies/Hz	$\omega 1 \geq 20$, $\omega 2 \geq 40$, $\omega 3 \geq 60$

Table 15.21 Optimized designs obtained for the planar 37-bar truss problem

Variable	Wang et al. [27]	Lingyun et al. [28]	Gomes [29]	Kaveh and Zolghadr			
				Standard CSS [30]	DPSO [32]	PSRO [33]	TWO [2]
Y3, Y19 (m)	1.2086	1.1998	0.9637	0.8726	0.9482	1.0087	1.0039
Y5, Y17 (m)	1.5788	1.6553	1.3978	1.2129	1.3439	1.3985	1.3531
Y7, Y15 (m)	1.6719	1.9652	1.5929	1.3826	1.5043	1.5344	1.5339
Y9, Y13 (m)	1.7703	2.0737	1.8812	1.4706	1.6350	1.6684	1.6768
Y11 (m)	1.8502	2.3050	2.0856	1.5683	1.7182	1.7137	1.7728
A1, A27 (cm^2)	3.2508	2.8932	2.6797	2.9082	2.6208	2.6368	2.8892
A2, A26 (cm^2)	1.2364	1.1201	1.1568	1.0212	1.0397	1.3034	1.0949
A3, A24 (cm^2)	1.0000	1.0000	2.3476	1.0363	1.0464	1.0029	1.0213
A4, A25 (cm^2)	2.5386	1.8655	1.7182	3.9147	2.7163	2.3325	2.6776
A5, A23 (cm^2)	1.3714	1.5962	1.2751	1.0025	1.0252	1.2868	1.1981
A6, A21 (cm^2)	1.3681	1.2642	1.4819	1.2167	1.5081	1.0704	1.1387
A7, A22 (cm^2)	2.4290	1.8254	4.6850	2.7146	2.3750	2.4442	2.6537
A8, A20 (cm^2)	1.6522	2.0009	1.1246	1.2663	1.4498	1.3416	1.4171
A9, A18 (cm^2)	1.8257	1.9526	2.1214	1.8006	1.4499	1.5724	1.3934
A10, A19 (cm^2)	2.3022	1.9705	3.8600	4.0274	2.5327	3.1202	2.7741
A11, A17 (cm^2)	1.3103	1.8294	2.9817	1.3364	1.2358	1.2143	1.2759
A12, A15 (cm^2)	1.4067	1.2358	1.2021	1.0548	1.3528	1.2954	1.2776
A13, A16 (cm^2)	2.1896	1.4049	1.2563	2.8116	2.9144	2.7997	2.1666
A14 (cm^2)	1.0000	1.0000	3.3276	1.1702	1.0085	1.0063	1.0099
Weight (kg)	366.50	368.84	377.20	362.84	360.40	360.97	360.27

Table 15.22 Natural frequencies (Hz) evaluated at the optimized designs for the planar 37-bar truss

Frequency number	Wang et al. [27]	Lingyun et al. [28]	Gomes [29]	Kaveh and Zolghadr			
				Standard CSS [30]	DPSO [32]	PSRO [33]	TWO [2]
1	20.0850	20.0013	20.0001	20.0000	20.0194	20.1023	20.0279
2	42.0743	40.0305	40.0003	40.0693	40.0113	40.0804	40.0146
3	62.9383	60.0000	60.0001	60.6982	60.0082	60.0516	60.0946
4	74.4539	73.0444	73.0440	75.7339	76.9896	75.8918	76.5062
5	90.0576	89.8244	89.8240	97.6137	97.2222	97.2470	96.5840

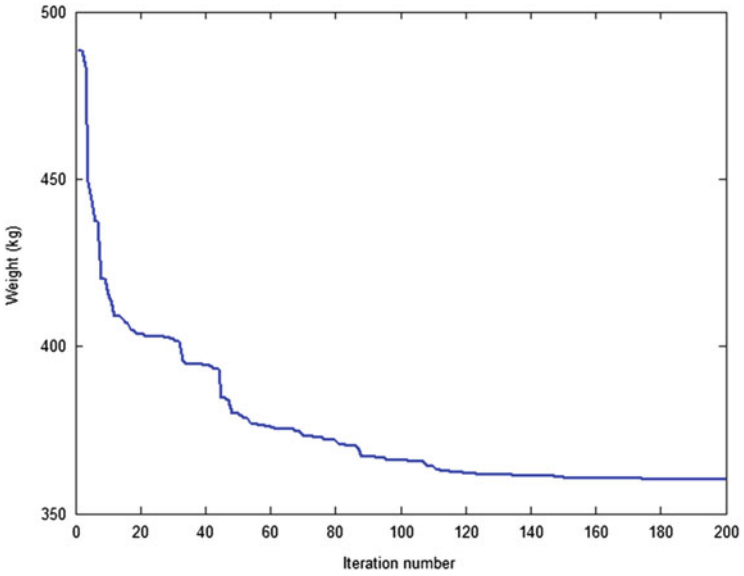

Fig. 15.13 Convergence curve of the best run of TWO for the simply supported 37-bar planar truss

a trap recognition capability [31], democratic PSO [32], and a hybridized PSRO algorithm [33].

Table 15.25 summarizes the best results obtained by different methods for this example. It can be seen that the structure found by TWO is lighter than those of other methods. The mean weight and the standard deviation of 50 independent runs of TWO are 214.25 kg and 12.64 kg, respectively. Table 15.26 shows the first five natural frequencies of the final structures found by various methods for the 52-bar dome-like space truss. The convergence curve of the best run of TWO for this problem is shown in Fig. 15.15.

15.5 Concluding Remarks

A newly proposed metaheuristic algorithm named tug of war optimization (TWO) [1] is presented and utilized for engineering optimization in this chapter. The algorithm considers each of the candidate solutions as a team competing in a series of rope-pulling competitions.

An idealized framework is presented in order to simplify the physical nature of a game of tug of war, in which the teams are considered as two bodies lying on a smooth surface. It is then assumed that the pulling force that a team can exert is proportional to its weight, and the two teams sustain their grip of the rope during the

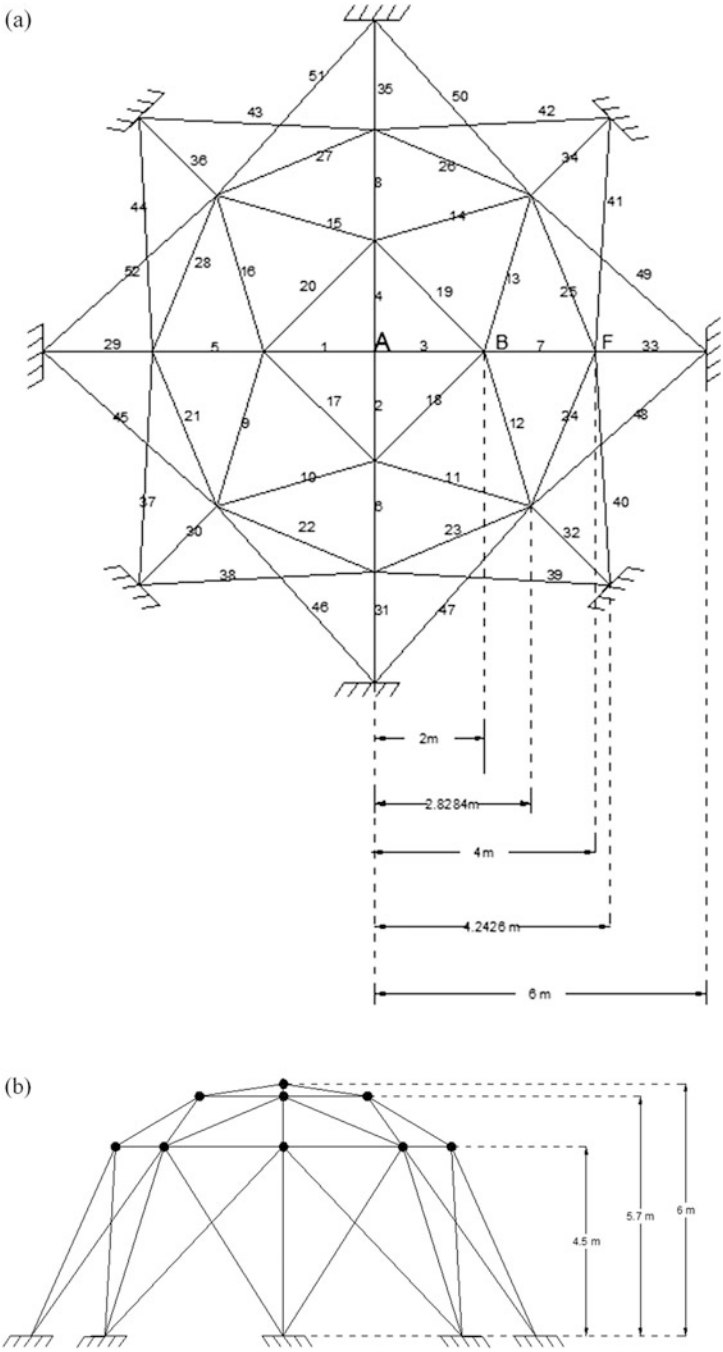

Fig. 15.14 Initial layout of the spatial 52-bar truss. (**a**) Top view. (**b**) Side view

Table 15.23 Material properties, frequency constraints, and variable bounds for the 52-bar space truss

Property/unit	Value
E (modulus of elasticity)/N/m^2	2.1×10^{11}
ρ (material density)/kg/m^3	7800
Added mass/kg	50
Allowable range for cross sections/m^2	$0.0001 \leq A \leq 0.001$
Constraints on the first three frequencies/Hz	$\omega_1 \leq 15.916$ $\omega_2 \geq 28.648$

Table 15.24 Element grouping for the spatial 52-bar truss

Group number	Elements
1	1–4
2	5–8
3	9–16
4	17–20
5	21–28
6	29–36
7	37–44
8	45–52

Table 15.25 Optimized designs obtained for the spatial 52-bar truss problem

				Kaveh and Zolghadr			
Variable	Lin et al. [34]	Lingyun et al. [28]	Gomes [29]	Standard CSS [30]	DPSO [32]	PSRO [33]	TWO [2]
Z_A (m)	4.3201	5.8851	5.5344	5.2716	6.1123	6.252	6.012
X_B (m)	1.3153	1.7623	2.0885	1.5909	2.2343	2.456	1.598
Z_B (m)	4.1740	4.4091	3.9283	3.7093	3.8321	3.826	4.287
X_F (m)	2.9169	3.4406	4.0255	3.5595	4.0316	4.179	3.641
Z_F (m)	3.2676	3.1874	2.4575	2.5757	2.5036	2.501	2.888
A1 (cm^2)	1.00	1.0000	0.3696	1.0464	1.0001	1.0007	2.1245
A2 (cm^2)	1.33	2.1417	4.1912	1.7295	1.1397	1.0312	1.1341
A3 (cm^2)	1.58	1.4858	1.5123	1.6507	1.2263	1.2403	1.1870
A4 (cm^2)	1.00	1.4018	1.5620	1.5059	1.3335	1.3355	1.3180
A5 (cm^2)	1.71	1.911	1.9154	1.7210	1.4161	1.5713	1.3637
A6 (cm^2)	1.54	1.0109	1.1315	1.0020	1.0001	1.0021	1.0299
A7 (cm^2)	2.65	1.4693	1.8233	1.7415	1.5750	1.3267	1.3479
A8 (cm^2)	2.87	2.1411	1.0904	1.2555	1.4357	1.5653	1.4446
Weight (kg)	298.0	236.046	228.381	205.237	195.351	197.186	194.25

Table 15.26 Natural frequencies of the optimized designs obtained for the spatial 52-bar truss problem

Frequency number	Lin et al. [36]	Lingyun et al. [28]	Gomes [29]	Kaveh and Zolghadr			
				Standard CSS [30]	DPSO [32]	PSRO [33]	TWO [2]
1	15.22	12.81	12.751	9.246	11.315	12.311	9.265
2	29.28	28.65	28.649	28.648	28.648	28.648	28.667
3	29.28	28.65	28.649	28.699	28.648	28.649	28.667
4	31.68	29.54	28.803	28.735	28.650	28.715	28.686
5	33.15	30.24	29.230	29.223	28.688	28.744	29.734

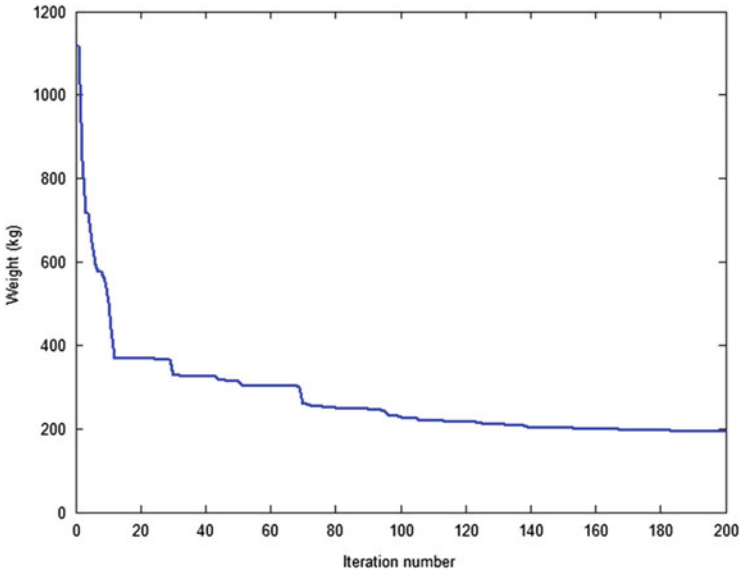

Fig. 15.15 Convergence curve of the best run of TWO for the 52-bar truss problem

contest. The weights of the teams are determined based on the quality of the solutions they represent.

Different numerical examples from various fields of structural optimization are investigated in order to show the viability and efficiency of TWO. Examples include truss weight minimization with static and dynamic constraints. Numerical results demonstrate that the proposed algorithm is a competent one, and its behavior is comparable to other state-of-the-art metaheuristic algorithms.

References

1. Kaveh A, Zolghadr A (2016) Tug of War Optimization: a new metaheuristic algorithm. Int J Optim Civil Eng 6(4):469–493
2. Kaveh A, Zolghadr A (2016) Truss shape and size optimization with frequency constraints using Tug of war optimization
3. Tsoulos IG (2008) Modifications of real code genetic algorithm for global optimization. Appl Math Comput 203:598–607
4. Belegundu AD (1982) A study of mathematical programming methods for structural optimization. Ph.D. thesis, Department of Civil and Environmental Engineering, University of Iowa, Iowa, USA
5. Arora JS (1989) Introduction to optimum design. McGraw-Hill, New York, NY
6. Coello CAC (2000) Use of a self-adaptive penalty approach for engineering optimization problems. Comput Indust 41:113–127
7. Coello CAC, Montes EM (2002) Constraint-handling in genetic algorithms through the use of dominance-based tournament selection. Adv Eng Inform 16:193–203
8. He Q, Wang L (2007) An effective co-evolutionary particle swarm optimization for constrained engineering design problems. Eng Appl Artific Intellig 20:89–99
9. Montes EM, Coello CAC (2008) An empirical study about the usefulness of evolution strategies to solve constrained optimization problems. Int J General Sys 37(4):443–473
10. Kaveh A, Talatahari S (2010) An improved ant colony optimization for constrained engineering design problems. Eng Comput 27(1):155–182
11. Kaveh A, Talatahari S (2010) A novel heuristic optimization method: charged system search. Acta Mech 213:267–289
12. Kaveh A, Mahdavi VR (2014) Colliding bodies optimization: a novel metaheuristic method. Comput Struct 139:18–27
13. Ragsdell KM, Phillips DT (1976) Optimal design of a class of welded structures using geometric programming. ASME J Eng Indust Ser B 98(3):1021–1025
14. Deb K (1991) Optimal design of a welded beam via genetic algorithms. AIAA J 29 (11):2013–2015
15. Rajeev S, Krishnamoorthy CS (1992) Discrete optimization of structures using genetic algorithms. ASCE J Struct Eng 118:1233–1250
16. Schutte JJ, Groenwold AA (2003) Sizing design of truss structures using particle swarms. Struct Multidisc Optim 25:261–269
17. Lee KS, Geem ZW (2004) A new structural optimization method based on the harmony search algorithm. Comput Struct 82:781–798
18. Erbatur F, Hasançebi O, Tütüncü I, Kiliç H (2000) Optimal design of planar and space structures with genetic algorithms. Comput Struct 75:209–224
19. Camp CV, Bichon J (2004) Design of space trusses using ant colony optimization. ASCE J Struct Eng 130:741–751
20. Perez RE, Behdinan K (2007) Particle swarm approach for structural design optimization. Comput Struct 85:1579–1588
21. Camp CV (2007) Design of space trusses using Big Bang–Big Crunch optimization. ASCE J Struct Eng 133:999–1008
22. Kaveh A, Khayatazad M (2012) A novel metaheuristic method: ray optimization. Comput Struct 112–113:283–294
23. Kaveh A, Talatahari S (2009) Particle swarm optimizer, ant colony strategy and harmony search scheme hybridized for optimization of truss structures. Comput Struct 87:267–283
24. Kaveh A, Ilchi Ghazaan M, Bakhshpoori T (2013) An improved ray optimization algorithm for design of truss structures. Period Polytech Civil Eng 57:97–112
25. Grandhi RV, Venkayya VB (1988) Structural optimization with frequency constraints. AIAA J 26(7):858–866

26. Sedaghati R, Suleman A, Tabarrok B (2002) Structural optimization with frequency constraints using finite element force method. AIAA J 40(2):382–388
27. Wang D, Zha WH, Jiang JS (2004) Truss optimization on shape and sizing with frequency constraints. AIAA J 42:1452–1456
28. Lingyun W, Mei Z, Guangming W, Guang M (2005) Truss optimization on shape and sizing with frequency constraints based on genetic algorithm. J Comput Mech 35(5):361–368
29. Gomes MH (2011) Truss optimization with dynamic constraints using a particle swarm algorithm. Exp Syst Appl 38(1):957–968
30. Kaveh A, Zolghadr A (2011) Shape and size optimization of truss structures with frequency constraints using enhanced charged system search algorithm. Asian J Civil Eng 12:487–509
31. Kaveh A, Zolghadr A (2012) Truss optimization with natural frequency constraints using a hybridized CSS-BBBC algorithm with trap recognition capability. Comput Struct 102–103:14–27
32. Kaveh A, Zolghadr A (2014) Democratic PSO for truss layout and size optimization with frequency constraints. Comput Struct 130:10–21
33. Kaveh A, Zolghadr A (2014) A new PSRO algorithm for frequency constraint truss shape and size optimization. Struct Eng Mech 52:445–468
34. Lin JH, Chen WY, Yu YS (1982) Structural optimization on geometrical configuration and element sizing with static and dynamic constraints. Comput Struct 15(5):507–515